Chitosan-Collagen Scaffolds with Nano/Microfibrous Architecture for Skin Tissue Engineering

Soumi Dey Sarkar,[a] Brooke L. Farrugia,[b] Tim R. Dargaville,[b] Santanu Dhara[a*]

a. School of Medical Science and Technology

Indian Institute of Technology Kharagpur

Kharagpur-721302, India

b. Institute of Health and Biomedical Innovation

Queensland University of Technology, Kelvin Grove

Queensland, 4059, Australia

[*]Corresponding Author: sdhara@smst.iitkgp.ernet.in, Tel. +91 3222 282306;

Fax: +91 3222 282221

Abstract

In this study, a hierarchical nano/microfibrous chitosan/collagen scaffold that approximates structural and functional attributes of native extracellular matrix (ECM), has been developed for applicability in skin tissue engineering. Scaffolds were produced by electrospinning of chitosan followed by imbibing of collagen solution, freeze-drying and subsequent cross-linking of two polymers. Scanning electron microscopy showed formation of layered scaffolds with nano/microfibrous architechture. Physico-chemical properties of scaffolds including tensile strength, swelling behavior and biodegradability were found satisfactory for intended application. 3T3 fibroblasts and HaCaT keratinocytes showed good *in vitro* cellular response on scaffolds thereby indicating the matrices' cytocompatible nature. Scaffolds tested in an *ex vivo* human skin equivalent (HSE) wound model, as a preliminary alternative to animal testing, showed keratinocyte migration and wound re-epithelization — a pre-requisite for healing and regeneration. Taken together, the herein proposed chitosan/collagen scaffold, shows good potential for skin tissue engineering.

Keywords: Nano/micro architecture, Chitosan, Collagen, Skin Tissue Engineering

1. Introduction

Native extracellular matrix (ECM) is a dynamic fibrillar network of self-assembled proteins and polysaccharides rather than a mere structural support for cells.[1,2] Acting as a reservoir for soluble cell signaling molecules, the ECM contributes enormously to tissue morphogenesis, homeostasis and regeneration.[3] The quest to understand both structural and functional attributes of ECM has motivated researchers to design materials with objective of mimicking matrices' architecture, physico-chemical properties, and biomolecular composition. The ultimate desired for these bioinspired templates is to induce cellular responses as natural ECM, with special emphasis on matrix's cell adhesion potential, biodegradability, and proteolytic susceptibility. Multi-scale fibrillar networks have been developed in recent times so as to mimic the ECM architecture and elucidate better cellular behavior. [4-7] Tuzlakoglu *et al.* explored the potential of nano/microfiber combined scaffolds, produced by electrospinning collagen onto starch-based fiber meshes for bone regeneration.[8] Results clearly indicated the significant role of collagen nanofibers in influencing viability and cytoskeletal organization of rat bone marrow stromal cells and human osteoblast-like cells. Similarly, by employing electrospun poly (ε-caprolactone) mats, with alternating micro and nanofibrous layers, Pham *et al*. showed enhanced spreading of rat marrow stromal cells on scaffolds.[9]

From the perspective of skin tissue engineering, a multi-scale fibrillar scaffold can be advantageous. Native human skin has a layered architecture with an overlying epidermis that contains keratinocytes, melanocytes, Merckl cells, and an underlying dermis that contains mainly fibroblasts within a fibrous connective tissue matrix. The two layers are mutually separated by an intermediate acellular glycoproteinacous basement membrane layer.[10] This layer is composed of protein microfilaments, containing collagen III/ IV/ VII, integrin, laminin

332, fibronectin and proteoglycans, along with other complex nanometer sized fibrous topographies that synchronously influence bio-chemical functionalities of native tissue. The underlying dermal layer comprises mostly of nano/microfibrous collagens, polysaccharides and water.[11] For the development of an engineered skin graft, it is essential to emulate the nano/micro-scalar fibrous architecture of tissue matrix and its biological cell recognition character. Combination of fabrication techniques like extrusion based rapid-prototyping, microfabrication, and spinning can be employed for reproducing architecture of ECM in scaffolds.[12-15] For reconstitution of the bio-adhesive character of ECMs, cell-recognizing domains can be introduced into scaffolds either by direct grafting of integrin binding units such as Arg-Gly-Asp (RGD), Asp-Gly-Glu-Ala (DGEA), or Tyr-Ile-Gly-Ser-Arg (YIGSR) onto surface-active polymers or by introducing adhesive motif rich proteins, usually collagen, fibronectin, or vitronectin.[16-18]

However, for successful skin regeneration, mimicking the architecture and biological cell recognition properties of ECM may not be adequate. Scaffolds should also provide critical functional roles like wound healing of native tissue matrix. Amongst the various stages involved in wound healing, closure of wound by migrating epithelial cells is crucial for restoration of intact epidermal barrier and protection of underlying tissue.[19] In some pathological conditions, like diabetic ulcers and third degree burns, re-epithelization is greatly hampered which may lead to development of non-healing chronic wounds. A significant apprehensive feature of chronic wounds is the presence of over-activated inflammatory cells that stimulate fibroblasts to secrete high level of matrix metalloproteinase (MMP).[11] This elevated MMP level not only denatures the non-viable collagen in wound beds, but also breaks down the viable collagen laid down by fibroblasts for granulation tissue formation.[11]

Additionally, fibroblasts at this stage fail to produce adequate levels of MMP inhibitors to restrict excess MMP activity.[20] Various cells (e.g. fibroblasts, endothelial cells) exist in senescent form and can hardly communicate with each other or function properly. All these events taken together restrict the formation of a suitable matrix needed for efficient cell migration and wound closure.[21]

A collagen based matrix can be promising in this regard for tackling issues of excess MMP activity by acting as a 'sacrificial substrate' in the wound.[22] Moreover, breakdown products of collagen are chemotactic for cells essential for granulation tissue formation.[23] Type I collagen being the major structural and functional protein of dermal matrix, migrating keratinocytes tend to interact with this protein and enhance collagenase production .[24] The collagenase thus produced in turn facilitates disassociation of keratinocytes from collagen rich substrates thereby allowing efficient keratinocyte migration over the provisional dermal matrix and effective wound closure .[21] However, in spite of its significant role in wound re-epithelization and healing, using just type I collagen for tissue engineering applications is restricted due to its fast biodegradation, poor mechanical properties and issues related to *in vivo* contraction.[25] In natural ECM, proteoglycans and glycosaminoglycans are usually coupled with collagen to provide mechanical stability and compressive strength.[26] Hereof, incorporation of chitosan, a glycosaminoglycan-like biodegradable polymer, into collagen based scaffolds may help in overcoming the potential limitations of collagen matrices. Chitosan, along with providing mechanical stability to collagen scaffolds, considerably contributes to the *in vitro* cellular response of chitosan/collagen scaffolds owing to its cytocompatible nature.[27] Moreover, the advantages that chitosan imparts to different aspects of wound healing, such as hemostasis,

antibacterial action and potential to accelerate collagen synthesis by fibroblasts, make it an attractive candidate for skin tissue engineering. [25, 28]

Various researchers have explored the potential of chitosan/collagen scaffolds for skin tissue engineering applications.[25, 29-30] However, not many studies have been directed towards the development of a scaffold with the wholesome approach of mimicking structural, biochemical and functional attributes of native tissue. Thus to address this highly demanding area of research, the present study aims to develop a layered nano/microfibrous chitosan/collagen scaffold thereby approximating structural hierarchy, organization, biochemical composition and functional features of native skin ECM. Sequential electrospinning and freeze-drying techniques have been employed for development of layered scaffolds with hierarchical fiber diameters and pore sizes. Freeze-dried nano/microfibrous layer with micron scale inter-fiber spacings may allow easy cellular migration and proliferation, thereby contributing to development of a functional dermal substitute. Nano-scalar pore size of electrospun layer, on the other hand, may control evaporative water loss, promote mass transport, and restrict invasion by exogenous microorganisms.[19]In order to evaluate *in vitro* cytocompatibility and appropriateness of scaffolds for skin tissue engineering, cellular responses of 3T3 fibroblasts and HaCaT keratinocytes were separately studied on freeze dried collagen layer and electrospun chitosan layer, respectively. In addition, the scaffolds were tested in *ex vivo* human skin equivalent (HSE) model, as a preliminary alternative to *in vivo* animal testing, so as to assess their re-epithelization and wound healing potential.

2. Materials and Methods

2.1 Fabrication of chitosan/collagen scaffolds

2.1.1 *Electrospinning of chitosan-PEO solution*

For this study, 3 wt % chitosan (average M_w ~ 710,000, <90% de-acetylated; Marine Chemicals, Kerala, India) and 10 wt % poly (ethylene oxide) (PEO, average M_w ~ 100,000; Sigma Aldrich, US) stock solutions, in 15M acetic acid, were used to prepare a 4:1 chitosan-PEO (w/w) blend (4C1P) for electrospinning. A 26 gauge blunt end stainless steel capillary needle was attached to a syringe containing 2 ml of 4C1P blend. Syringe was placed on a syringe pump (KD Scientific, Switzerland) that allowed precise control of solution flow rates in micro-liter range. Needle was connected to positive electrode of a high voltage DC power supply (30 kV, Glass Mann, Japan). A grounded cylindrical collector (6 cm diameter), wrapped in aluminum foil and rotating at 200 rpm, was placed at a tip-to-collector distance of 15 cm. Flow-rate of 8 µL/min, 20 kV DC voltage were maintained throughout electrospinning process carried out at room temperature. Electrospun 4C1P mat was immersed in 5 wt % aqueous sodium-tripolyphosphate (STPP, Loba Chem Mumbai, India) bath (pH 7) for 5 mins for ionotropic crosslinking of chitosan with tri-polyphosphates. This also facilitated easy retrieval of samples from foil surface. PEO and unreacted TPP were removed by incubation in aqueous medium at 37°C for 5 days under shaking condition.[31] Cross-linked samples (referred as Chi-CL) were air dried on a Teflon coated plate overnight.

2.1.2 *Freeze-drying of type I collagen on electrospun mats*

Collagen type I, used in this study, was extracted from scales of *Labeo rohita* using a two step demineralization and salting out process as reported by Pati *et al.*[32,33] 1 mg/ml of type I collagen solution was obtained by dissolving freeze-dried collagen in 0.5 M acetic acid and

overnight stirring at 4 °C. To obtain collagen fibers, the solution was further dialyzed against 0.1M acetic acid and distilled water for 24 hours to attain pH ~ 6. Collagen solution was poured over Chi-CL mats, placed in rectangular molds, and frozen at -80 °C for 24 hrs followed by overnight lyophilization at -45 °C. The mats obtained (Chi-CL-Col) were treated with aqueous N-hydroxysuccinimide (NHS)/1-ethyl-3-(3-dimethylaminopropyl) carbodiimide (EDC) (SRL Pvt. Ltd, Mumbai, India) solution (pH 5.5) to crosslink collagen.[34] The NHS-EDC treated lyophilized samples thus obtained are referred as Chi-CL-Col-CL. Two different sides of Chi-CL-Col-CL scaffolds containing the electrospun layer and collagen rich layer are labeled as Chi-CL-Col-CL/U and Chi-CL-Col-CL/D, respectively.

2.2 Physico-chemical characterisation of scaffolds

2.2.1 Scanning electron microscopy

Morphologies of Chi-CL, Chi-CL-Col and Chi-CL-Col-CL scaffolds were analyzed using scanning electron microscope (SEM, EVO 60/Zeiss, Germany) at an accelerating voltage of 10-20 kV. The fully dried scaffolds were gold-coated (Polaron sputter coater) at 40 mA for 90 s prior to observation under SEM. Average fiber diameters were determined from SEM micrographs of 20 randomly chosen fibers using IT3 software (University of Texas Health Centre, San Antonio, US).

2.2.2 Porosity determination

To determine porosity of scaffolds, fully dried Chi-CL and Chi-CL-Col-CL samples were cut into rectangular pieces. The mass (W_1) and volume (V_1) of each sample were recorded prior to immersion in pycnometer filled with absolute alcohol. After 2 hours of immersion masses of saturated samples (W_2) were recorded. Porosities of scaffolds were determined from equation (1).

$$\% \text{ Porosity} = (W_2 - W_1) / (\rho V_1) \times 100 \quad (1)$$

where ρ is the density of ethanol at 25 °C (= 789 kg/m³)

2.2.3 ATR/FTIR spectroscopy

ATR/FTIR spectra of the scaffolds and collagen powder were recorded using a Thermo Nicolet spectrophotometer (Model – NEXUS-870, Thermo Nicolet Corporation, Madison, WI, USA) with ZnSe crystal ATR accessory. For Chi-CL-Col-CL samples, ATR spectra of both sides (i.e. Chi-CL-Col-CL/U and Chi-CL-Col-CL/D) were recorded. For freeze-dried collagen powder, pellets were prepared along with KBr and FTIR spectra was recorded in transmission mode. All spectra were recorded from 500-4000 cm^{-1}.

2.2.4 Swelling behavior

Chi-CL, Chi-CL-Col and Chi-CL-Col-CL scaffolds of known dry masses (W_d) were incubated in PBS at 37 °C for 24 hours. Swollen weights (W_w) of scaffolds were recorded at different time intervals until equilibrium. Swelling ratio of scaffolds was obtained from equation (2).

$$\% \text{ Swelling} = [(W_w - W_d)/W_d] \times 100 \quad (2)$$

2.2.5 Biodegradation kinetics

In vitro biodegradation behaviour of collagen (Col), Chi-CL-Col and Chi-CL-Col-CL scaffolds of were studied by collagenase digestion, as reported by Ma *et al*.[25] In brief, the samples were incubated in PBS supplemented with 100 mg/ml (28 units) collagenase type I (Himedia, Mumbai, India) at 37°C for 4, 12, 24 and 72 h. At specific time intervals, the degradation was discontinued by incubating the sample mixture in ice bath followed by centrifugation at 1500 rpm for 10 min. The supernatant obtained was hydrolyzed with 6mM HCl at 120 °C for 12 h. The hydroxyproline content was assessed using UV spectroscopy. The

biodegradation degree of scaffolds is defined as percentage of hydroxyproline released at specific times to the fully degraded sample having same composition and weight.

2.2.6 Mechanical properties

Tensile properties of Chi-CL, Chi-CL-Col and Chi-CL-Col-CL scaffolds (n=5 for each) were evaluated through mechanical testing (Model H25KS, Hounsfield, UK) under tensile mode using a 25 N load-cell with cross-head speed of 0.5 mm/min. Scaffolds were sectioned into thin strips (~ 5 mm width, ~ 0.008 and 0.1 mm thickness for Chi-CL and Chi-CL-Col-CL, respectively) and clamped onto tensile grips. Initial gauge length of 10 mm was maintained for each test.

2.3 *In vitro* cell culture using 3T3 fibroblasts and HaCaT keratinocytes

3T3 fibroblast and HaCaT keratinocyte cells (obtained from NCCS, Pune) were maintained in humidified environment (37 °C, 5% CO_2) and cultured in Dulbecco's modified Eagle's medium (DMEM; Himedia, Mumbai, India) with 10 % fetal bovine serum (FBS; Himedia, Mumbai, India) and 1% antibiotic agent (Himedia, Mumbai, India). For *in vitro* cell culture study, Chi-CL and Chi-CL-Col-CL scaffolds were cut into 8 mm diameter discs. Prior to cell seeding, scaffolds were sterilized using 70% ethanol for 3 hrs, washed repeatedly with phosphate buffered saline (PBS) followed by overnight incubation in cell culture medium. 3T3 fibroblasts were seeded onto the collagen rich layer of Chi-CL-Col-CL scaffold (i.e. Chi-CL-Col-CL/U) at a density of 1 x 10^5 cells / scaffold. A similar density of HaCaT keratinocytes were seeded on electrospun chitosan based layer (i.e. Chi-CL-Col-CL/D) of another set of Chi-CL-Col-CL scaffolds. Cells were also seeded onto Chi-CL scaffolds and tissue culture polystyrene (TCP; positive control) for comparative analysis. The samples were incubated at 37 °C and culture medium was replaced every 24 hours.

2.3.1 Observation under SEM

SEM microscopy was performed to evaluate morphological characteristics of proliferating 3T3 fibroblast and HaCaT keratinocytes seeded on scaffolds. After 1 and 7 days of culture, the cells were fixed in 2.5% glutaraldehyde for 30 min at 4°C followed by rinsing and dehydration in ascending series of aqueous ethanol (50–100%). To ensure complete drying, the samples were further vacuum dried and observed under SEM following conditions outlined in section 2.2.1.

2.3.2 Cell viability assay

Viability of 3T3 and HaCaT cells seeded on Chi-CL and Chi-CL-Col-CL scaffolds were assessed using live / dead viability/ cytotoxicity kit (Molecular Probes, Invitrogen, Eugene, OR, USA) following the manufacturer's protocol. Briefly, cell-seeded scaffolds were washed thoroughly in PBS to remove traces of serum-supplemented DMEM medium. 1 mL of solution containing 2 µM calcein AM and 4 µM ethidium homodimer-1 was added to each sample and incubated for 30–45 min at room temperature. Samples were further washed thoroughly to avoid background staining and visualized under fluorescent microscope (Zeiss, Germany) with suitable filters. Live cell cytoplasm on staining emitted a green fluorescence while dead cell nuclei were stained red.

Viable cell proliferation on Chi-CL, Chi-CL-Col-CL scaffolds and TCP were quantified using MTT assay using 3T3 and HaCaT cells, as reported by Datta *et al.*[35] After 1, 3 and 7days of cell seeding, media was removed and samples were washed repeatedly with PBS followed by incubation in 5 mg/mL of MTT (3-(4, 5-Dimethylthiazol-2-yl)-2, 5-diphenyltetrazolium bromide, Sigma, US) solution at 37 ºC for 4 h. The insoluble formazan crystals were dissolved in DMSO by shaking for 30 mins. A standard curve was prepared using suspensions with known

number of cells, determined by an automated cell counter (Countess, Invitrogen). Absorbance was recorded at 570 nm using a Platescreen (RMS, Chandigarh, India).

2.4 Application of scaffolds on *ex vivo* human skin equivalent (HSE) wound model

To investigate the wound healing potential, Chi-CL and Chi-CL-Col-CL scaffolds were tested on an *ex vivo* human skin equivalent (HSE) model (n=3). HSEs were prepared from skin samples, collected from consenting patients undergoing elective abdominal and breast reduction surgeries, using a method reported by Xie *et al.*[36] Ethics approval was obtained from Queensland University of Technology Review Board prior to skin collection. The study was carried out with strict adherence to Declaration of Helsinki Principles. Initially, keratinocytes were isolated from epidermal layer of skin and cultured in Full Green's medium. For isolation of fibroblasts, the dermal pieces were immersed in DMEM medium (Invitrogen) with 0.05% collagenase A (type I; Invitrogen, Mulgrave, Australia) at 37 ° C, 5% CO_2 for 18 h followed by centrifugation. The cells obtained were maintained in FBS supplemented DMEM medium. Decellulalrised de-epidermised dermis (DED) was prepared using a technique, reported by Dawson *et al.*[37] For preparation of DED-HSEs, sterile stainless steel rings having an inner diameter of 6.7 mm were placed onto the papillary side of each DED piece (1.8 cm × 1.8 cm) and 2×10^{4} number fibroblasts were seeded onto the matrix inside the ring. The samples were incubated for 72 hours prior to seeding of keratinocytes on top of fibroblasts. The samples were incubated for 48 hours followed by lifting to air-liquid interface. After 7 days of maintaining the samples at air-liquid interface, full thickness wounds (4 mm diameter) were created in HSEs by cutting through epidermal and dermal layers using a biopsy punch (Stiefel, North Carolina, USA), followed by removal of incised core. Chi-CL and Chi-CL-Col-CL scaffolds were also cut into 4 mm diameter discs using biopsy punch before stacking them into the incised wound in HSEs. Wounded HSEs

were probed using histology after 14 d of application of scaffolds. Samples were thus fixed in 4% neutral buffered formalin, followed by paraffin embedding, serial sectioning, hematoxylin and eosin staining and visualization under a Nikon Eclipse TE2000-U microscope equipped with Photometrics cool snap LS camera.

2.5 Statistical analysis

The results are presented here as mean ± standard deviation. Comparisons were made using Origin Pro8 software for paired t-tests and at 95% confidence intervals ($p < 0.05$) significant difference were asserted.

3. Results and discussion

3.1. Scaffold morphology

Chitosan/collagen scaffolds with hierarchical nano/microfiber architecture were successfully developed by sequential electrospinning, freeze-drying and subsequent cross-linking. Primarily, randomly aligned nanofiber mats with ~78 nm fiber diameter, ~ 81 % porosity, and nano-scale inter-fiber spacing were prepared by electrospinning chitosan/PEO blend. This was followed by cross-linking of nanofibers by TPP ions in order to stabilize their architecture in an aqueous/acidic medium (Fig 1a). Further, TPP cross-linked nanofiber (Chi-CL) mats were used as base materials on which type I collagen solution (~ pH 6) was freeze-dried to form layered scaffold architecture with multi-scale fiber diameters (0.3-15 μm) (Fig.1b). Fig. 1c and d represents two different layers of Chi-CL-Col scaffolds- the lower collagen based thick porous layer with submicron scale fiber diameters and upper chitosan based nanofibrous layer, respectively. Here it is to be noted that, the upper chitosan based nanofibrous layer was also partially covered with collagen fibers due to flowability of collagen solution prior to freeze drying. Actually, the collagen fibers, in the different layers of Chi-CL-Col scaffolds, were

formed during dialysis and subsequent freeze drying due to inherent amphiphilic property of the collagen molecules that facilitated fibrillogenesis by self-assembly at pH close to isoelectric point.[38] Furthermore, these chitosan-collagen based scaffolds (Chi-CL-Col), having ~200 μm thickness, were crosslinked by NHS-EDC so as to tailor their degradation and improve mechanical integrity under *in vitro* conditions. Crosslinking of scaffolds caused insignificant microstructural changes and allowed retention of ~ 61% interconnected porosity, as in uncrosslinked ones.

3.2. ATR/FTIR analysis

ATR/FTIR spectra of collagen powder, Chi-CL, Chi-CL-Col, and either sides of Chi-CL-Col-CL scaffolds (i.e. Chi-CL-Col-CL/U, and Chi-CL-Col-CL/D) are shown in Fig. 2a. The spectra of Chi-CL, Chi-CL-Col, Chi-CL-Col-CL/U, and Chi-CL-Col-CL/D showed characteristic chitosan peaks for amide I at ~ 1640 cm^{-1} (C=O stretching), amide II at ~1534 cm^{-1} (N-H in plane deformation), amide III at ~1380 cm^{-1} and saccharide unit at 898 cm^{-1}. The spectra for collagen powder showed peaks at ~ 3318 cm^{-1} (amide A; N–H stretching), ~1640 cm^{-1} (amide I; C=O stretching), ~1534 cm^{-1} (amide II; N–H deformation). The peak intensities for Chi-CL-Col scaffold at ~ 1640 cm^{-1} (amide I) and ~1534 cm^{-1} (amide II) increased due to incorporation of collagen as expected. Further increase in peak intensities of amide I and amide II bands in Chi-CL-Col-CL/U and Chi-CL-Col-CL/D spectra signifies successful NHS-EDC cross-linking though inter/intra molecular amide linkage in hybrid polymeric scaffold. While comparing the spectra of Chi-CL-Col-CL/D and Chi-CL-Col-CL/U, higher intensity amide I and II bands in the former indicated higher collagen content in the lower layer of Chi-CL-Col-CL scaffold.

3.3. Swelling and biodegradation of scaffolds

A scaffold with appreciable swelling property is desirable for wound healing application as it can absorb moisture from exudating wound beds. Fig. 2b represents swelling behavior of Chi-CL, Chi-CL-Col and Chi-CL-Col-CL scaffolds in PBS (pH ~ 7.4) at 37^{o}C. The Chi-CL scaffolds showed rapid swelling (~ 300 %) and attained equilibrium within first hour of incubation. On the other hand, Chi-CL-Col and Chi-CL-Col-CL took approximately 12 and 22 hours, respectively to reach equilibrium. This may be attributed to greater water absorption capacity of porous collagen layer in Chi-CL-Col and Chi-CL-Col-CL scaffolds. The crosslinked chitosan-collagen scaffolds (Chi-CL-Col-CL) exhibited lesser swelling (~ 450 %) than the uncross-linked Chi-CL-Col scaffolds (~ 600 %) thereby manifesting their higher stability in aqueous medium.

While considering a matrix for tissue engineering application, besides its swelling property, degradation kinetics is also vital. In this study, biodegradation degree of collagen (Col), Chi-CL-Col and Chi-CL-Col-CL was investigated in collagenase medium at 37°C (Fig. 2c). The uncross-linked type I collagen showed ~ 91% biodegradation in 4 hours and was completely degraded by 12 hours study period. The uncross-linked Chi-CL-Col scaffolds also underwent a rapid 44% degradation within 72 hour study period. The NHS/EDC cross-linked Chi-CL-Col-CL scaffolds showed relatively higher stability (~16% degradation in 72 h) which can be attributed to enhanced inter and intra-molecular interaction between parent polymers through carbodiimide mediated covalent cross-linking.

3.4. Tensile properties

Mechanical properties of an engineered scaffold play important roles in imparting stability during tissue integration and neo-tissue formation. The tensile properties of Chi-CL,

Chi-CL-Col and Chi-CL-Col-CL were determined and presented in Fig. 2d. Tensile strength of Chi-CL, Chi-CL-Col and Chi-CL-Col-CL were recorded as 5.9 ± 0.28 MPa, 6.96 ± 0.54 MPa and 7.59 ± 0.61 MPa, respectively. These high tensile strengths of scaffolds are associated with their fibrous architecture and large number of inter-fiber crossover points giving rise to intrinsic cohesive force. In case of Chi-CL-Col and Chi-CL-Col-CL scaffolds, the higher strengths in comparison to Chi-CL scaffolds are mainly due to incorporation of collagen fibrils and their intermolecular interactions with chitosan nanofibers as described in section 3.2. Elongation at break of Chi-CL, Chi-CL-Col and Chi-CL-Col-CL scaffolds were found to be 9.08 ± 0.67%, 13.11 ± 0.58%, and 8.54 ± 2.1%, respectively. Incorporation of collagen microfibrils into chitosan based nanofiber network allowed significantly higher elongation ($p < 0.05$) of resultant samples (Chi-CL-Col) prior to failure mainly due to considerable inter-chain slippage under tension. However, marked reduction in elongation at break of NHS-EDC treated Chi-CL-Col scaffold (Chi-CL-Col-CL) was attributed to carbodiimide mediated cross-linking of chitosan and collagen that caused inter-fiber locking and restricted inter-chain slippage. Further, elastic modulus of Chi-CL, Chi-CL-Col, and Chi-CL-Col- CL scaffolds were recorded as 134.1±15.2 MPa, 150.1±12.4 MPa, and 174.9±7.9 MPa, respectively. The results clearly indicated improvement in tensile properties of scaffolds due to collagen incorporation and subsequent NHS-EDC mediated crosslinking.

3.5 Cell culture and cytocompatibility of scaffolds

Attachment, viability, and proliferation of cells on scaffolds are crucial to assess matrix cytocompatibility and are prerequisites for any tissue engineering application. Adhesion/proliferation potentials of 3T3 fibroblasts and HaCaT keratinocytes on Chi-CL and Chi-CL-Col-CL scaffolds were evaluated by SEM at different time points after cell seeding. As

observed in SEM micrographs (Fig. 3), both scaffolds supported cell adhesion and growth of 3T3 and HaCaT cells. After the first day of incubation, attachment of cells and their subsequent elongation was higher on Chi-CL-Col-CL scaffold (Fig. 3a, c). The cells also developed lamelipodial protrusions by day 1 on Chi-CL-Col-CL scaffold. For Chi-CL scaffolds, after similar incubation time, cells remained clustered and round shaped with non-spread morphology (Fig.3 b, d). This difference in initial cellular response between two scaffolds may be attributed to presence of collagen on Chi-CL-Col-CL scaffolds. RGD domains of collagen present high affinity chemotactic focal adhesion points to cells that cause integrin up-regulation, cascades intracellular signaling/transcription and promotes good initial cell attachment.[39] The reason for better cellular elongation on Chi-CL-Col-CL scaffolds may be attributed to higher porosity and interconnectivity in collagen layer that facilitated easier cell distribution and movement. However after 7 d of incubation, both 3T3 and HaCaT cells underwent significant proliferation (as also observed from MTT assay) on both Chi-CL and Chi-CL-Col-CL scaffolds, along with development of extensive lamelipodial protrusions which may be indicative of good cell-material interactions (Fig. 3e, f, g, h).[40] For Chi-CL scaffolds, nanofibers acted as positive stimuli after initial attachment phase and supported enhanced cell spreading and formation of a sheath like morphology by day 7. On the other hand, for Chi-CL-Col-CL scaffolds, nano/microfibers of collagen provided geometrical and biological signals for effective cell proliferation, distribution and migration due to their structural and biochemical resemblance with protein's supramolecular arrangement in native environment.

Viability of 3T3 fibroblasts and HaCaT keratinocyte cells on Chi-CL, Chi-CL-Col-CL scaffolds and TCP were assessed qualitatively and quantitatively after 1, 3 and 7 days, using live/dead assay and MTT assay respectively (Fig. 4). Results showed between two scaffolds,

Chi-CL-Col-CL exhibited superior cellular response, in terms of better initial attachment by 1day (121 ± 36 3T3 fibroblasts/ mm^2; 62 ± 16 HaCaT keratinocytes/ mm^2), rapid proliferation and viability after 3days (453 ± 20 3T3 fibroblasts/mm^2; 194 ± 30 HaCaT keratinocytes/mm^2), and 7days (760 ± 26 3T3 fibroblasts/mm^2; 591 ± 42 HaCaT keratinocytes/ mm^2). Conversely, cells grown on Chi-CL scaffolds showed comparatively less initial attachment after 1day of incubation (8 ± 5 3T3 fibroblasts/mm^2; 20 ± 15 HaCaT keratinocytes/ mm^2), and comparatively inferior cell viability after 3days (293 ± 45 3T3 fibroblasts/mm^2; 132 ± 20 HaCaT keratinocytes/mm^2) and 7days (460 ± 74 3T3 fibroblasts/mm^2; 401 ± 43 HaCaT keratinocytes/mm^2). The significant difference ($p < 0.05$) in cellular viability on two scaffolds may be attributed to their disparity in initial cell adhesion properties due to presence of collagen. Good initial adherence has often been associated with superior cell viability in later stages, as also evident for Chi-CL-Col-CL scaffolds in this study.[41] In comparison to the scaffolds, though TCP showed better cell adhesion after 1day of incubation (210 ± 56 3T3 fibroblasts/mm^2; 168 ± 40 HaCaT keratinocytes/mm^2), this difference was reduced after 3 days (505 ± 74 3T3 fibroblasts/mm^2; 398± 67 HaCaT keratinocytes/mm^2) and 7 days (546 ± 130 3T3 fibroblasts/mm^2; 371 ± 40 HaCaT keratinocytes/mm^2). The viable cell count on TCP was comparable on Chi-CL-Col-CL and Chi-CL after 3 and 7 days, respectively. In fact after 7days of incubation, viable cell count on Chi-CL-Col-CL was significantly higher than that of TCP ($p < 0.05$), essentially due to the three-dimensional architecture of scaffolds providing relatively higher surface area. Cell proliferation rate on TCP, on the other hand, reduced after 3 days due to stagnancy in cellular growth caused by contact inhibition.

3.6 Wound healing potential of scaffolds

An essential feature of wound healing and regeneration lies in restoration of intact epidermal barrier through re-epithelization. Controlled proliferation and directed migration of keratinocytes through dermal/provisional matrix is critical for re-epithelization and disparity in this function often relates to non-healing wounds.[19] The present study evaluated potential of Chi-CL and Chi-CL-Col-CL for re-epithelization and healing of full-thickness wounds in an *ex vivo* HSE model, as a preliminary alternative to animal testing (Fig. 5). Fig. 5 a, b and c represent the HSE model prior to any defect, after wound creation and application of scaffolds to wound, respectively. MTT staining of HSEs with Chi-CL, after 14 days of application, showed characteristic purple color development on surrounding HSE matrix but not on scaffolds signifying absence of viable cells in wound region (Fig. 5d). Histology results showed minimal number of Chi-CL discs were retained in HSE wounds after 14 days (Fig. 5e). However, the Chi-CL discs that were retained in wound hardly supported any keratinocyte migration or re-epithelization. On the other hand for HSE wounds with Chi-CL-Col-CL, MTT staining showed typical purple color development on scaffolds and adjacent HSE after 14 days, thereby indicating presence of viable cells (Fig. 5f). Histology results clearly indicated keratinocyte migration through Chi-CL-Col-CL and re-epithelization of HSE wounds after 14 days of scaffold application (Fig. 5g). The inset of Fig. 5 g shows development of stratified epidermis over HSE wounds with Chi-CL-Col-CL scaffolds. This enhanced re-epithelization potential of Chi-CL-Col-CL may be attributed to presence of type I collagen in scaffold. Type I collagen provides binding and cleavage sites for collagenase I (MMP I), a matrix metalloproteinase whose optimal catalytic activity is vital for wound healing.[42] Following an injury, MMP I facilitates removal of degraded ECM components in a wound and re-organizes the provisional matrix for efficient

keratinocyte migration.[24] MMP I expression is consistently induced by primary keratinocytes, migrating across the wound bed, only when cells are in contact with type I collagen and not with basement membrane proteins or with other components of wound bed.[24] Moreover, cleavage of type I collagen provides keratinocytes with a mechanism to maintain their directionality during re-epithelization. The above mentioned finding from previous reports, taken together, explains the defect closure phenomenon in HSEs with Chi-CL-Col-CL scaffolds. Chi-CL scaffolds being devoid of collagen could not necessarily direct the MMP I production and keratinocyte migration. MMP I, that are produced by keratinocytes in wound boundary, did not get suitable binding and cleavage sites in Chi-CL scaffolds and hence could not maintain cellular migration necessary for re-epithelization..

As also observed from histology results, both Chi-CL and Chi-CL-Col-CL scaffolds facilitated minimal/no fibroblast migration and related ECM synthesis which restricted complete healing of full-thickness wounds. The probable reason for such a phenomenon may be absence of macrophages in HSE model, that secrete pro-inflammatory cytokines (eg .TNF- α, IL-1bβ) responsible for fibroblast mediated collagen synthesis and deposition in wound.[21] It is anticipated that, application of scaffolds in an animal model may provide a better insight to their full-thickness wound healing potential, due to presence of suitable cells, cytokines and growth factors present *in vivo*. Results also indicated that stacks of scaffold discs could not be fitted optimally in wound thereby decreasing their stability during healing and further histological processing (Fig. 5g). Air spaces occluded the scaffold stacks and hence it became difficult to set up a three dimensional bridge with interconnected porosity so as to facilitate fibroblast migration into wound (inset of Fig. 5g). In order to overcome stability and stacking related limitations, current research is being directed in our laboratory towards development of three-dimensional plug like

scaffolds, closely mimicking the thickness of native skin. Possibilities of using cytocompatible glues are also being explored in order to ensure that scaffolds remain in contact and adhered to wound edges and bed. *Ex vivo* and *in vivo* wound re-epithelization and healing studies are also being carried out using 3-D chitosan/collagen plug scaffolds, and will be reported.

4. Conclusions

The present work demonstrates successful development of chitosan-collagen scaffolds with hierarchical nano/microfiber architecture as a support matrix for wound healing and skin tissue engineering applications. Physico-chemical properties of prepared scaffolds were found suitable for intended purpose. 3T3 fibroblasts and HaCaT keratinocytes cultured on chitosan-collagen based scaffolds showed superior cellular response in comparison to the ones without collagen. Our results also demonstrate that topical application of these chitosan-collagen scaffolds in human skin equivalent models can promote keratinocyte migration and re-epithelization in full thickness wounds. Such topical mode of action is promising for skin tissue engineering applications, as they hold potential to overcome the persistent problem of full thickness wound healing and regeneration.

Acknowledgements Authors would like to acknowledge Mr. Nantu Dogra for help in experiments, Dept. of Science and Technology, India for financial support, IIT Kharagpur and the Tissue Repair and Regeneration Program, Queensland University of Technology` for infrastructural facilities and Mr. Debashish Mishra for proof-reading the manuscript.

References

1. Martins A, Pinho ED, Correlo VM, Faria S, Marques AP, Reis RL, Neves NM. Biodegradable nanofibers-reinforced microfibrous composite scaffolds for bone tissue engineering. Tissue Eng Part A 2010;12:3599-609.
2. Badylak SF, Freytes DO, Gilbert TW. Extracellular matrix as a biological scaffold material: Structure and function. Acta Biomater 2009;5:1-13.
3. Teti A. Regulation of cellular functions by extracellular matrix. J Am Soc Nephrol 1992; 2(10 Suppl):S83-7.
4. Murtuza B, Nichol JW, Khademhosseini A. Micro- and nanoscale control of the cardiac stem cell niche for tissue fabrication. Tissue Eng Part B Rev. 2009; 15:443-54.
5. Mota C, Puppi D, Dinucci D, Errico C, Bártolo P, Chiellini F. Dual-Scale Polymeric Constructs as Scaffolds for Tissue Engineering. Materials 2011;4:527-542.
6. Park SH, Kim TG, Kim HC, Yang DY, Park TG. Development of dual scale scaffolds via direct polymer melt deposition and electrospinning for applications in tissue regeneration. Acta Biomater 2008;4:1198-207.
7. Soliman S, Pagliari S, Rinaldi A, Forte G, Fiaccavento R, Pagliari F, Franzese O, Minieri M, Di Nardo P, Licoccia S, Traversa E. Multiscale three-dimensional scaffolds for soft tissue engineering via multimodal electrospinning. Acta Biomater2010;6:1227-37.
8. Tuzlakoglu K, Bolgen N, Salgado AJ, Gomes ME, Piskin E, Reis RL. Nano- and micro-fiber combined scaffolds: a new architecture for bone tissue engineering. J Mater Sci Mater Med 2005;16:1099-104.
9. Pham QP, Sharma U, Mikos AG. Electrospun Poly(E-caprolactone) Microfiber and Multilayer Nanofiber/Microfiber Scaffolds: Characterization of Scaffolds and Measurement of Cellular Infiltration. Biomacromolecules 2006;7:2796-805.
10. Tobin DJ.Biochemistry of human skin—our brain on the outside. Chem Soc. Rev 2006;35:52-67.
11. Fitzgerald RH, Steinberg JH.Collagen in Wound Healing: Are We Onto Something New or Just Repeating the Past? The Foot and Ankle Online Journal 2009;2.

12. Chen R, Morsi Y, Patel S, Ke Q-F, Mo X-M.A novel approach via combination of electrospinning and FDM for tri-leaflet heart valve scaffold fabrication. Front Mater Sci China 2009;3:359-366.
13. Downing BR, Cornwell K, Toner M, Pins GD. The influence of microtextured basal lamina analog topography on keratinocyte function and epidermal organization. J Biomed Mater Res A 2005;72:47-56.
14. Shanjani Y, Hu Y, Pilliar RM, Toyserkani E. Mechanical characteristics of solid-freeform-fabricated porous calcium polyphosphate structures with oriented stacked layers. Acta Biomater 2011;7:1788-96.
15. Wan Y, Cao X, Zhang S, Wang S, Wu Q. Fibrous poly(chitosan-g-dl-lactic acid) scaffolds prepared via electro-wet-spinning. Acta Biomater 2008;4:876-86.
16. Kim TG, Park TG. Biomimicking extracellular matrix: cell adhesive RGD peptide modified electrospun poly(D,L-lactic-co-glycolic acid) nanofiber mesh. Tissue Eng 2006; 12:221-33.
17. Shachar M, Tsur-Gang O, Dvir T, Leor J, Cohen S. The effect of immobilized RGD peptide in alginate scaffolds on cardiac tissue engineering Acta Biomater 2011; 7:152-62.
18. Ragetly G, Griffon DJ, Chung YS.The effect of type II collagen coating of chitosan fibrous scaffolds on mesenchymal stem cell adhesion and chondrogenesis. Acta Biomater 2010;6:3988-97.
19. Schneider A, Wang XY, Kaplan DL, Garlick JA, Egles C. Biofunctionalized electrospun silk mats as a topical bioactive dressing for accelerated wound healing. Acta Biomater 2009;5:2570-8.
20. Cao Y, Croll T, Rizzi SC, Shooter GK, Edwards H, Finlayson K, Upton Z, Dargaville TR. Hydrogel Tethered Inhibitor of MMPs. J Biomed Mater Res A 2011; 96A:663-72.
21. Brett D. http://www.woundsresearch.com/content/a-review-collagen-and-collagen-based-wound-dressings?page=0,1. February 15,2012.
22. Rangaraj A, Harding K, Leaper D. Role of collagen in wound management. Wounds 2011; 7:54-63.
23. Schultz G, Mast B. Molecular analysis of the environment of healing and chronic wounds: cytokines, proteases and growth factors. Wounds 1998;10 (6 suppl):1F-9F.

24. Pilcher BK, Dumin JA, Sudbeck BD, Krane SM, Welgus HG, Parks WC. The Activity of Collagenase-1 Is Required for keratinocyte migration on a type I collagen matrix. J Cell Biol 1997;137:1445-57.

25. Ma L, Gao C, Mao Z, Zhou J, Shen J, Hu X, Han C. Collagen/chitosan porous scaffolds with improved biostability for skin tissue engineering. Biomaterials 2003;24: 4833–4841

26. Schultz GS, Ladwig G, Wysocki A. http://www.worldwidewounds.com/2005/august/Schultz/Extrace-Matric-Acute-Chronic-Wounds.html. February 19,2012.

27. Tsai S-P, Hsieh C-Y, Hsieh C-Y, Wang D-M, Huang LL-H, Lai J-Y, Hsieh H-J. Preparation and Cell Compatibility Evaluation of Chitosan/Collagen Composite Scaffolds Using Amino Acids as Crosslinking Bridges. J Appl Polym Sc 2007; 105:1774-1785.

28. Park CJ, Clark SG, Lichtensteiger CA, Jamison RD, Johnson AJ. Accelerated wound closure of pressure ulcers in aged mice by chitosan scaffolds with and without bFGF. Acta Biomater 2009;5:1926-36.

29. Ma L, Gao C, Mao Z, Zhou J, Shen J, Hu X, Han C. Collagen/chitosan porous scaffolds with improved biostability for skin tissue engineering. Biomaterials 2003;24:4833-41.

30. Han CM, Zhang LP, Sun JZ, Shi HF, Zhou J, Gao CY. Application of collagen-chitosan/fibrin glue asymmetric scaffolds in skin tissue engineering. J Zhejiang Univ Sci B 2010;11:524-30.

31. Jeong SI, Krebs MD, Bonino CA, Khan SA, Alsberg E. Electrospun Alginate Nanofibers with Controlled Cell Adhesion for Tissue Engineering. Macromol Biosci 2010;10:934-43.

32. Pati F, Adhikari B, Dhara S. Isolation and characterization of fish scale collagen of higher thermal stability. Bioresour Technol 2010; 101:3737-42.

33. Pati F, Adhikari B, Dhara S. Collagen scaffolds derived from fresh water fish origin and their biocompatibility. J Biomed Mater Res A 2012;100A:1068-1079.

34. Olde Damink LH, Dijkstra PJ, van Luyn MJ, van Wachem PB, Nieuwenhuis P, Feijen J. In vi&o degradation of dermal sheep collagen cross-linked using a watersoluble carbodiimide. Biomaterials 1996;17:679-684.

35. Datta P, Dhara S, Chatterjee J. Hydrogels and electrospun nanofibrous scaffolds of N-methylene phosphonic chitosan as bioinspired osteoconductive materials for bone grafting. Carbohydr Polym 2012; 87:1354-62.
36. Xie Y, Rizzi SC, Dawson R, Lynam E, Richards S, Leavesley DI, Upton Z. Development of a Three-Dimensional Human Skin Equivalent Wound Model for Investigating Novel Wound Healing Therapies. Tissue Eng Part C Methods 2010;16:1111-23.
37. Dawson RA, Upton Z, Malda J, Harkin DG. Preparation of cultured skin for transplantation using insulin-like growth factor I in conjunction with insulin-like growth factor binding protein 5, epidermal growth factor, and vitronectin. Transplantation 2006; 81:1668-76.
38. Jiang F, Hörber H, Howard J, Müller DJ. Assembly of collagen into microribbons: effects of pH and electrolytes. J Struct Biol 2004; 148:268-78.
39. Cavalcanti-Adam EA, Volberg T, Micoulet A, Kessler H, Geiger B, Spatz JP. Cell Spreading and Focal Adhesion Dynamics Are Regulated by Spacing of Integrin Ligands. Biophys J 2007; 92:2964-74.
40. Pati F, Adhikari B, Dhara S. Collagen Intermingled Chitosan-Tripolyphosphate Nano/Micro Fibrous Scaffolds for Tissue-Engineering Application. J Biomater Sci Polym Ed 2011; In Press.
41. Lee J, Kang BS, Hicks B, Chancellor TF Jr, Chu BH, Wang HT, Keselowsky BG, Ren F, Lele TP.The control of cell adhesion and viability by zinc oxide nanorods. Biomaterials 2008;29:3743-9.
42. Riley KN, Herman IM.Collagenase Promotes the Cellular Responses to Injury and Wound Healing In Vivo. J Burns Wounds 2005;4:e8.

736 List of figures

Figure No	Caption
Fig. 1	SEM micrographs of (a) electrospun 4:1 chitosan/PEO nanofibers treated with STPP (Chi-CL), (d)cross-sectional view of layered chitosan-collagen scaffolds (Chi-CL-Col) ; (c) Lower collagen rich layer of Chi-CL-Col scaffolds (d) Upper electrospun chitosan/freeze-dried collagen based layer of Chi-CL-Col scaffolds.
Fig. 2	(a) ATR/FTIR spectra of STPP treated chitosan based nanofibers (Chi-CL), collagen powder, chitosan-collagen scaffolds (Chi-CL-Col) and either sides of NHS-EDC treated chitosan-collagen (Chi-CL-Col-CL) scaffolds i.e. Chi-CL-Col-CL/U and Chi-CL-Col-CL/D; (b) Swelling behavior of Chi-CL, Chi-CL-Col and Chi-CL-Col-CL ; (c) *In vitro* biodegradation behavior of collagen (Col), Chi-CL-Col and Chi-CL-Col-CL and (d) Tensile properties of Chi-CL, Chi-CL-Col and Chi-CL-Col-CL.
Fig. 3	SEM micrographs showing attachment and proliferation of 3T3 fibroblasts and HaCaT keratinocytes on STPP treated chitosan based nanofiber (Chi-CL) and NHS-EDC treated chitosan-collagen scaffolds (Chi-CL-Col-CL) scaffolds after 1 and 7 days. Upper and lower layers of Chi-CL-Col-CL scaffolds have been labeled as Chi-CL-Col-CL/U and Chi-CL-Col-CL/D. (a,b) 3T3 fibroblasts on Chi-CL-Col-CL/D and Chi-CL , respectively after 1 d; (c,d) HaCaT keratinocytes on Chi-CL-Col-CL/U and Chi-CL, respectively after 1 d; (e,f) 3T3 fibroblasts on Chi-CL-Col-CL/D and Chi-CL, respectively after 7d; (g,h) HaCaT keratinocytes on Chi-CL-Col-CL/U and Chi-CL, respectively after 7d.
Fig. 4	Fluorescent microscopic images of Calcein AM/ Ethidium homodimer stained 3T3 fibroblasts and HaCaT keratinocytes on STPP treated chitosan based nanofiber (Chi-CL)

	and NHS-EDC treated chitosan-collagen scaffolds (Chi-CL-Col-CL) scaffolds after 1, 3 and 7 days. Upper and lower layers of Chi-CL-Col-CL scaffolds have been labeled as Chi-CL-Col-CL/U and Chi-CL-Col-CL/D. (a,b) 3T3 fibroblasts on Chi-CL-Col-CL/D and Chi-CL , respectively after 1 d; (c,d) HaCaT keratinocytes on Chi-CL-Col-CL/U and Chi-CL, respectively after 1 d; (e,f) 3T3 fibroblasts on Chi-CL-Col-CL/D and Chi-CL, respectively after 3 d; (g,h) HaCaT keratinocytes on Chi-CL-Col-CL/U and Chi-CL, respectively after 3d.; (i,j) 3T3 fibroblasts on Chi-CL-Col-CL/D and Chi-CL, respectively after 7 d; (k,l) HaCaT keratinocytes on Chi-CL-Col-CL/U and Chi-CL, respectively after 7d ; (m,n) viable cell count on Chi-CL-Col-CL, Chi-CL scaffolds and tissue culture polystyrene (TCP) after 1, 3 and 7 days using 3T3 fibroblasts and HaCaT keratinocytes, respectively.
Fig. 5	Optical images of (a) Human skin equivalent model (HSE), (b) wound created on HSE, (c) Scaffolds placed on wounded HSE (d) MTT stained STPP treated chitosan based nanofiber scaffolds (Chi-CL) after 14 d in wounded HSE (d) Light microscopic images of H&E stained HSE wound after 14 d of treatment with STPP treated chitosan based nanofibrous scaffold (Chi-CL) (at 4X magnification) , (e) Digital image of MTT stained NHS-EDC treated chitosan-collagen scaffolds (Chi-CL-Col-CL) after 14 d in wounded HSE, (f) Light microscopic image of H&E stained NHS-EDC treated chitosan-collagen scaffolds (Chi-CL-Col-CL) after 14 d in wounded HSE (at 4X magnification). The inset of (f) represents of 10 X magnified image of selected area (shown by dotted square).

737

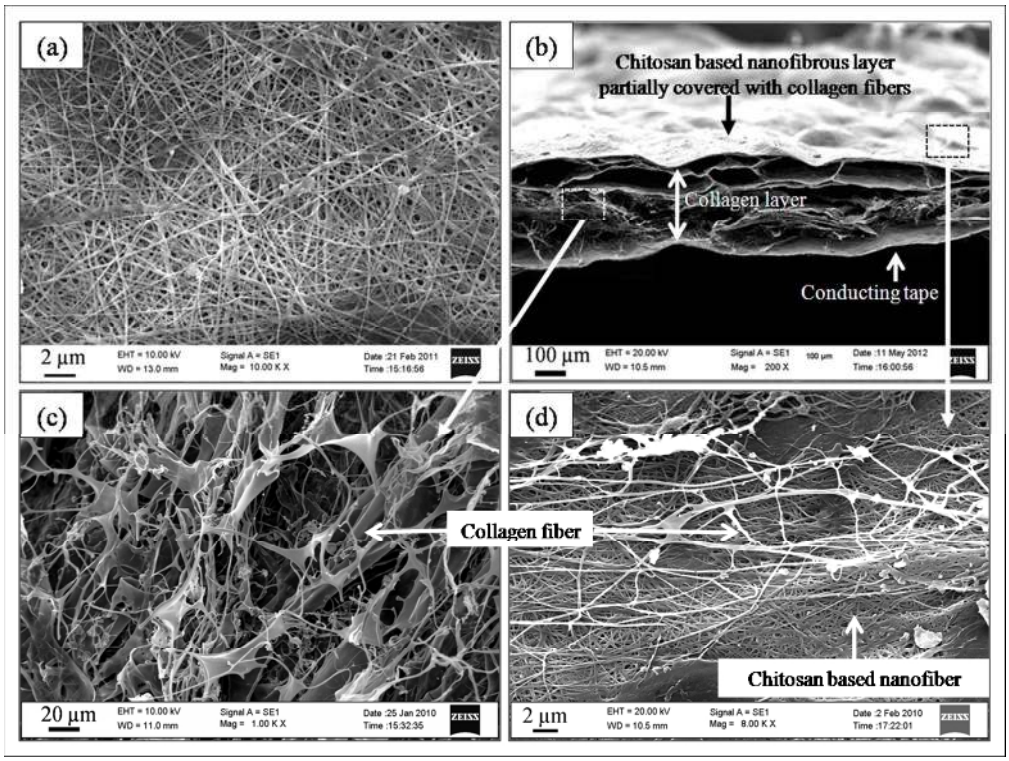

Fig 1. SEM micrographs of (a) electrospun 4:1 chitosan/PEO nanofibers treated with STPP (Chi-CL), (d)cross-sectional view of layered chitosan-collagen scaffolds (Chi-CL-Col) ; (c) Lower collagen rich layer of Chi-CL-Col scaffolds (d) Upper electrospun chitosan/freeze-dried collagen based layer of Chi-CL-Col scaffolds.
101x76mm (300 x 300 DPI)

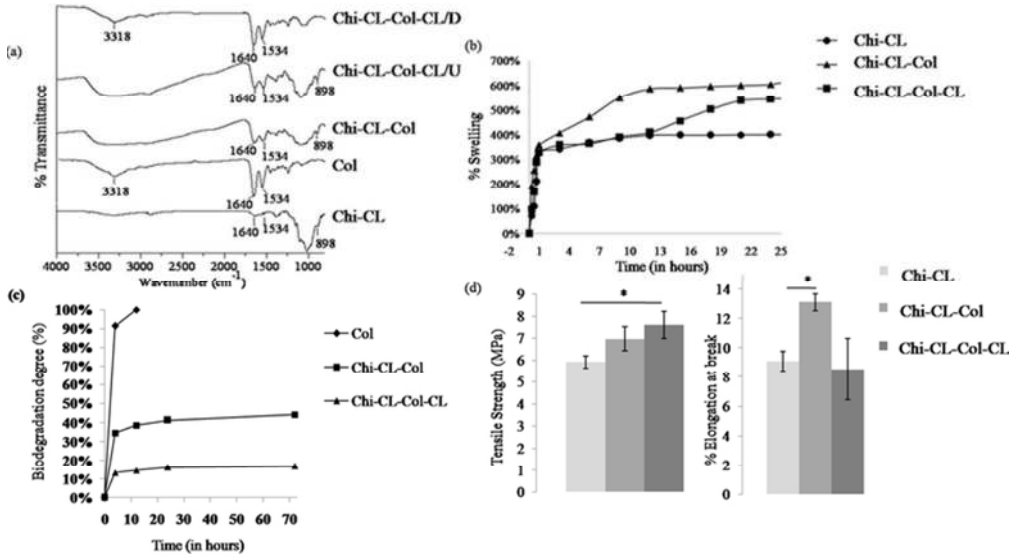

Fig 2. (a) ATR/FTIR spectra of STPP treated chitosan based nanofibers (Chi-CL), collagen powder, chitosan-collagen scaffolds (Chi-CL-Col) and either sides of NHS-EDC treated chitosan-collagen (Chi-CL-Col-CL) scaffolds i.e. Chi-CL-Col-CL/U and Chi-CL-Col-CL/D; (b) Swelling behavior of Chi-CL, Chi-CL-Col and Chi-CL-Col-CL ; (c) In vitro biodegradation behavior of collagen (Col), Chi-CL-Col and Chi-CL-Col-CL and (d) Tensile properties of Chi-CL, Chi-CL-Col and Chi-CL-Col-CL.
63x35mm (300 x 300 DPI)

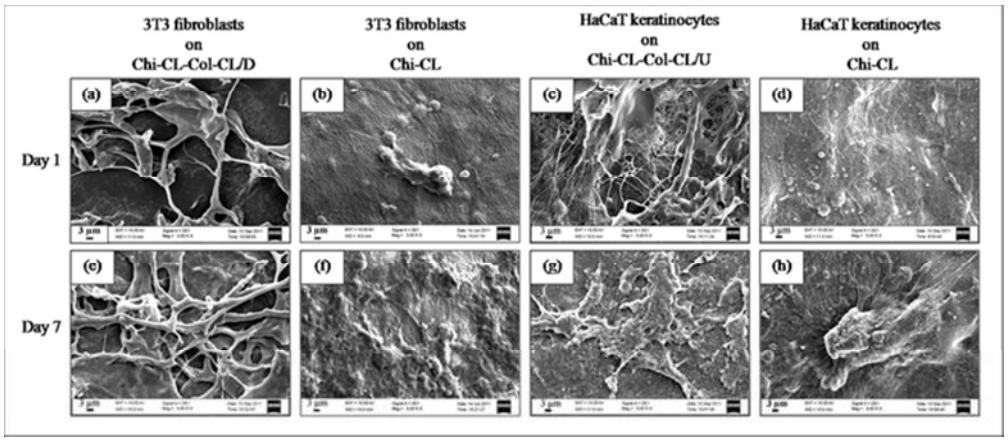

Fig 3.SEM micrographs showing attachment and proliferation of 3T3 fibroblasts and HaCaT keratinocytes on STPP treated chitosan based nanofiber (Chi-CL) and NHS-EDC treated chitosan-collagen scaffolds (Chi-CL-Col-CL) scaffolds after 1 and 7 days. Upper and lower layers of Chi-CL-Col-CL scaffolds have been labeled as Chi-CL-Col-CL/U and Chi-CL-Col-CL/D. (a,b) 3T3 fibroblasts on Chi-CL-Col-CL/D and Chi-CL , respectively after 1 d; (c,d) HaCaT keratinocytes on Chi-CL-Col-CL/U and Chi-CL, respectively after 1 d; (e,f) 3T3 fibroblasts on Chi-CL-Col-CL/D and Chi-CL, respectively after 7d; (g,h) HaCaT keratinocytes on Chi-CL-Col-CL/U and Chi-CL, respectively after 7d.
57x24mm (300 x 300 DPI)

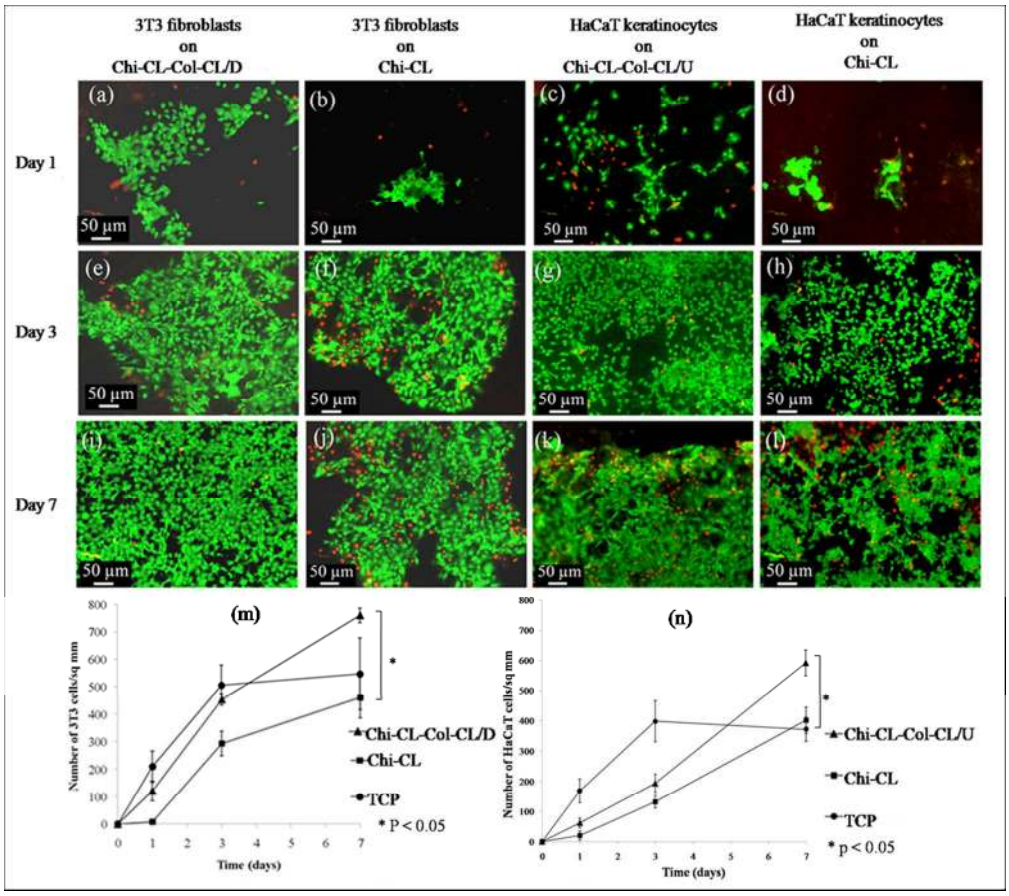

Fig 4. Fluorescent microscopic images of Calcein AM/ Ethidium homodimer stained 3T3 fibroblasts and HaCaT keratinocytes on STPP treated chitosan based nanofiber (Chi-CL) and NHS-EDC treated chitosan-collagen scaffolds (Chi-CL-Col-CL) scaffolds after 1, 3 and 7 days. Upper and lower layers of Chi-CL-Col-CL scaffolds have been labeled as Chi-CL-Col-CL/U and Chi-CL-Col-CL/D. (a,b) 3T3 fibroblasts on Chi-CL-Col-CL/D and Chi-CL , respectively after 1 d; (c,d) HaCaT keratinocytes on Chi-CL-Col-CL/U and Chi-CL, respectively after 1 d; (e,f) 3T3 fibroblasts on Chi-CL-Col-CL/D and Chi-CL, respectively after 3 d; (g,h) HaCaT keratinocytes on Chi-CL-Col-CL/U and Chi-CL, respectively after 3d.; (i,j) 3T3 fibroblasts on Chi-CL-Col-CL/D and Chi-CL, respectively after 7 d; (k,l) HaCaT keratinocytes on Chi-CL-Col-CL/U and Chi-CL, respectively after 7d ; (m,n) viable cell count on Chi-CL-Col-CL, Chi-CL scaffolds and tissue culture polystyrene (TCP) after 1, 3 and 7 days using 3T3 fibroblasts and HaCaT keratinocytes, respectively.
104x92mm (300 x 300 DPI)

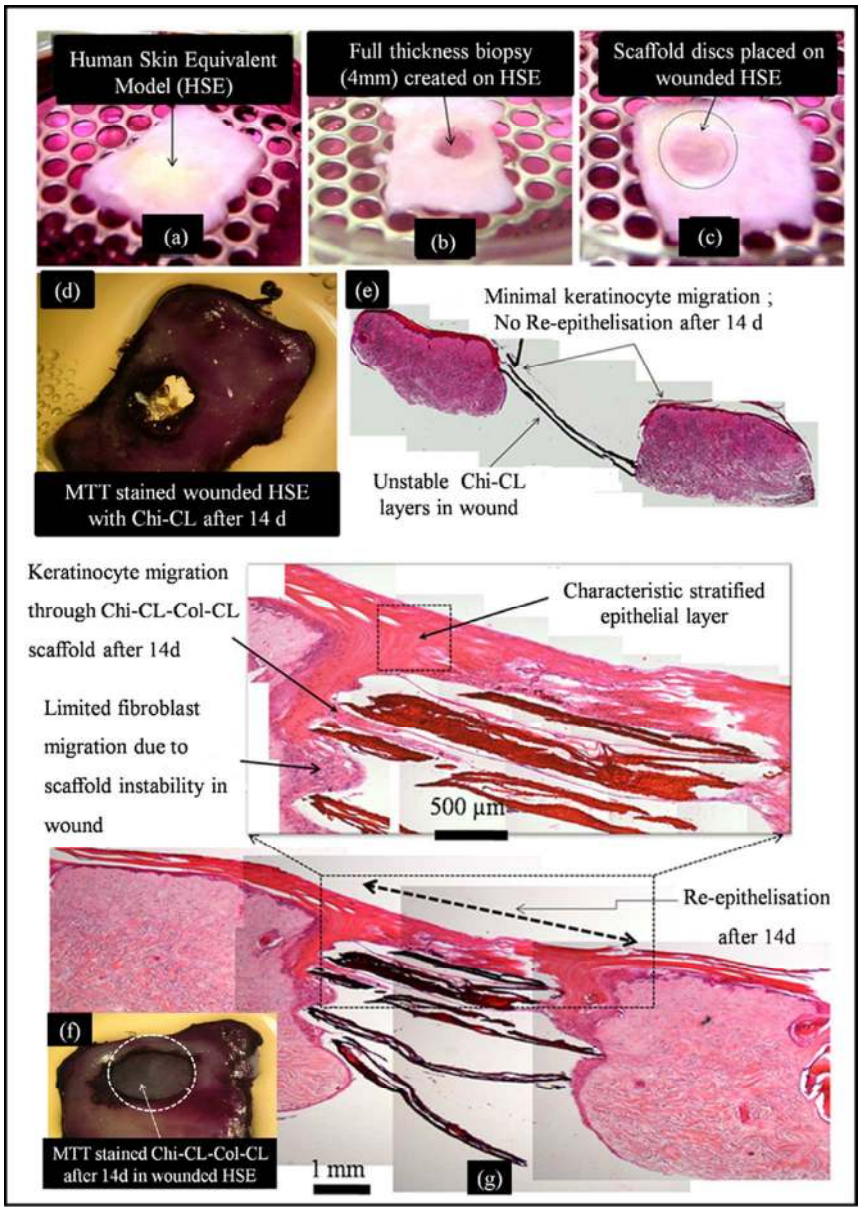

Fig 5. Optical images of (a) Human skin equivalent model (HSE), (b) wound created on HSE, (c) Scaffolds placed on wounded HSE (d) MTT stained STPP treated chitosan based nanofiber scaffolds (Chi-CL) after 14 d in wounded HSE (d) Light microscopic images of H&E stained HSE wound after 14 d of treatment with STPP treated chitosan based nanofibrous scaffold (Chi-CL) (at 4X maginification) , (e) Digital image of MTT stained NHS-EDC treated chitosan-collagen scaffolds (Chi-CL-Col-CL) after 14 d in wounded HSE, (f) Light microscopic image of H&E stained NHS-EDC treated chitosan-collagen scaffolds (Chi-CL-Col-CL) after 14 d in wounded HSE (at 4X maginification). The inset of (f) represents of 10 X magnified image of selected area (shown by dotted square).
132x186mm (300 x 300 DPI)